UNIVERSITY
OF TRENTO

DIPARTIMENTO DI INGEGNERIA E SCIENZA DELL'INFORMAZIONE

38123 Povo – Trento (Italy), Via Sommarive 14
http://www.disi.unitn.it

RAY PROPAGATION IN NONUNIFORM RANDOM LATTICES – PART II

A. Martini, R. Azaro, M. Franceschetti, and A. Massa

August 2007

Technical Report # DISI-11-065

Ray propagation in nonuniform random lattices - Part II

Anna Martini

Department of Information and Communication Technology, University of Trento, via Sommarive 14, I-38050 Trento, Italy

Renzo Azaro

Department of Information and Communication Technology, University of Trento, via Sommarive 14, I-38050 Trento, Italy

Massimo Franceschetti

Department of Electrical and Computer Engineering, University of California at San Diego, 9500 Gilman Drive, La Jolla, California 92093-0407

Department of Information and Communication Technology, University of Trento, via Sommarive 14, I-38050 Trento, Italy

Andrea Massa

Department of Information and Communication Technology, University of Trento, via Sommarive 14, I-38050 Trento, Italy

Ray propagation in nonuniform random lattices - Part II

Anna Martini, Renzo Azaro, Massimo Franceschetti, and Andrea Massa

Abstract

In this paper and its companion, the problem of ray propagation in nonuniform random half-plane lattices is considered. Cells can be independently occupied according to a density distribution that depends on the lattice depth. An electromagnetic source external to the lattice radiates a monochromatic plane wave that undergoes specular reflections on the occupied sites. The probability of penetrating up to level k inside the lattice is analytically evaluated by means of two different approaches, the former applying the theory of Markov chains (Markov approach) and the latter using the theory of Martingale random processes (Martingale approach). The full theory concerned with the Martingale approach is presented here, along with an innovative modification that leads to some improved results. Numerical experiments show that it outperforms the Markov approach when dealing with ray propagation in dense lattices described by a slowly varying density profile.

OCIS codes: 000.3860, 000.5490, 030.6600, 080.2710, 350.5500.

1 Introduction

This paper deals with ray propagation in nonuniform half-plane random lattices [1][2], where each site can be independently occupied with probability $q_j = 1 - p_j$, j being the row index. A monochromatic plane wave impinges on the lattice with a prescribed angle θ. Sites are assumed to be large compared to the wavelength, and accordingly the incident wave is modeled as a collection of parallel rays that undergo specular reflections on the occupied cells, see Figure 1. The objective is to analytically estimate the probability, $\Pr\{0 \longmapsto k\}$, that a single ray reaches a prescribed level k inside the lattice before being reflected back in the above empty half-plane.

The companion paper [3] provided a solution based on the so-called Markov (MKV) approach, which is summarized next. The original bi-dimensional ray propagation problem is recast as a one-dimensional random-walk problem, where the dependence on the incidence angle θ is lost. The core observation is that whenever a ray hits an occupied vertical face it does not change its vertical direction of propagation. Thus, from the point of view of evaluating the propagation depth, only reflections on horizontal faces play a relevant role and at each level the ray runs into just one of them, independently from θ. A ray traveling with positive direction inside level j either enters level $j+1$, keeping its direction of propagation, or it remains in the level j, changing its directions of propagation. These two mutually exclusive events clearly depend on the status of the encountered horizontal face, which is occupied with probability q_{j+1}. Similar considerations hold true when a ray traveling inside level j with negative direction is considered, but in this case the two events occur on the basis of the occupancy probability at level $j-1$. Accordingly, ray propagation inside the whole lattice is described by means of a Markov chain [4], leading to the following result (see [3] for details),

$$\Pr\{0 \longmapsto k\} = \frac{p_1 p_2}{1 + p_1 p_2 \sum_{i=0}^{k-3} \frac{q_{k-i}}{p_{k-i} p_{k-i-1}}}, \tag{1}$$

which reduces to

$$\Pr\{0 \longmapsto k\} = \frac{p^2}{(k-2)q+1}, \tag{2}$$

when the special case $q_j = q$ for all j is considered. It is also worth reminding that in order to construct the Markov chain, it is assumed that the ray never crosses cells it has already encountered along its path. This assumption lose validity when the incidence angle is far from 45^o and when the percolation lattice is dense. The solution provided by (1) and (2) has been exhaustively compared with that proposed in [5], which is limited to uniform random lattices having $q_j = q$ for all j, and to its extension to the nonuniform case, briefly summarized in [3], and referred to as the Martingale (MTG) approach.

This paper supplements [3] by presenting in detail the theory of the MTG approach, along with a mathematical analysis on the range of validity of the proposed solution that was not provided in [3]. Moreover, a modification that leads to improved results is proposed and compared to the MKV approach. It is shown that this modified version of the MTG approach outperforms the MKV approach when dealing with dense random grids described by slowly varying density profiles.

The paper is organized as follows. In Section 2, the MTG approach is carefully presented. The range of validity of the proposed solution is carefully discussed in Section 3. Section 4 deals with the numerical validation, providing a comparison between the MTG and the MKV approaches with reference to an exhaustive number of tests concerned with various density profiles as well as incidence angle conditions. Final comments and conclusions are drawn in Section 5.

2 Martingale Approach

The propagation of a ray inside the lattice is described by a realization of the following one-dimensional stochastic process [Fig. $1(a)$]:

$$r_n = r_0 + \sum_{m=1}^{n} x_m, \qquad n \geq 0, \tag{3}$$

where r_n is the lattice row reached after $n+1$ reflections, r_0 is the row where the first reflection takes place, and

$$x_n = r_n - r_{n-1}, \qquad n \geq 1, \tag{4}$$

is a sequence modeling the change of level between successive reflections. According to such a formulation, the probability that a single ray reaches level k before being reflected back into the above empty half-plane can be denoted as $\Pr\{r_N \geq k\}$, where N is the number of jumps such that the ray either reaches (and possibly goes beyond) the level k [Fig. $2(a)$] or it is reflected back crossing level 0 [Fig. $2(b)$], i.e.,

$$N = \min\{n : \ r_n \geq k \ or \ r_n \leq 0\}. \tag{5}$$

Now, let us express $\Pr\{r_N \geq k\}$ as follows:

$$\Pr\{r_N \geq k\} = \sum_{i=0}^{\infty} \Pr\{r_N \geq k \,|r_0 = i\} \Pr\{r_0 = i\}, \tag{6}$$

where $\Pr\{r_0 = i\}$ is the probability mass function of r_0 (i.e., the probability that the first reflection takes place at level i, $i \geq 0$) and the remaining term $\Pr\{r_N \geq k \,|r_0 = i\}$ represents the probability, conditioned to r_0, that the ray reaches level k before escaping in the above empty half-plane.

As far as $\Pr\{r_0 = i\}$ is concerned, two mutually-exclusive situations can occur. The ray impinging on the lattice is reflected either at level $i = 0$, without entering the half-plane,

or at a level $i \geq 1$. In the first case,

$$\Pr\{r_0 = 0\} = q_1, \tag{7}$$

q_1 being the occupancy probability of the first level. Otherwise, under the assumption of cell-status independence, $\Pr\{r_0 = 0\}$ is computed as the product of the following three probabilities: (a) the probability that the ray enters the lattice, $\Pr\{a\} = p_1$, (b) the probability that any cell on the ray' s path until level i is empty, $\Pr\{b\}$, and (c) the probability that a reflection takes place at level i given that the ray has freely crossed the previous $i-1$ levels, $\Pr\{c\}$. Since, at every level j, the ray runs into $\tan\theta$ vertical faces[1] (with overall probability $p_j^{tan\theta}$ to be empty) and one horizontal face (statistically characterized by the probability p_{j+1} to be empty), we have,

$$\Pr\{b\} = \prod_{j=1}^{i-1} p_{e_j}^{+}, \tag{8}$$

where $p_{e_j}^{+} = p_j^{tan\theta} p_{j+1}$ is the effective probability that the ray, proceeding in the positive direction, crosses level j reaching level $j+1$. As far as $\Pr\{c\}$ is concerned, a reflection takes place at level i if one of the following situations occurs: the first vertical face reached by the ray, which proceeds towards level i, is occupied; this face is empty and the ray hits the next one; and so on until the ray completes its path of length $\tan\theta$ and is reflected by the horizontal face separating level i and level $i+1$. Accordingly,

$$\Pr\{c\} = q_i \sum_{s=0}^{\tan\theta - 1} p_i^s + q_{i+1} p_i^{\tan\theta} = 1 - p_{e_i}^{+} = q_{e_i}^{+}. \tag{9}$$

[1] When a single stochastic process realization is considered, such a value should be rounded to an integer, but in our case, focusing on average propagation properties, the real value is considered.

Combining the previous results, we obtain

$$\Pr\{r_0 = i\} = \begin{cases} q_1, & i = 0, \\ p_1 q_{e_i}^+ \prod_{j=1}^{i-1} p_{e_j}^+, & i \geq 1. \end{cases} \tag{10}$$

Computation of $\Pr\{r_N \geq k \,|r_0 = i\}$ is now in order. Let us point out that three mutually-exclusive situations can occur: (a) $r_0 = 0$, (b) $0 < r_0 < k$, and (c) $r_0 \geq k$. While cases (a) and (c) are trivial, a deeper analysis is required to evaluate $\Pr\{r_N \geq k \,|r_0 = i\}$ when dealing with the case (b). Let us introduce the shifted version, with respect to the level r_0, of the process (3), that is

$$r'_n = r_n - r_0 = \sum_{m=1}^{n} x_m, \quad n \geq 1. \tag{11}$$

Under the ansatz that the ray jumps following the first one (x_n, $n \geq 1$) are independent and zero-mean, the stochastic process $\{r'_n,\ n \geq 1\}$ can be considered a *martingale* [6] with respect to $\{x_n,\ n \geq 1\}$ (see **Appendix A**). Therefore, following the same procedure described in [5], we obtain

$$\Pr\{r_N \geq k \,|r_0 = i\} = \frac{-\langle r'_N \,|r'_N \leq -r_0 \rangle}{\langle r'_N \,|r'_N \geq k - r_0 \rangle - \langle r'_N \,|r'_N \leq -r_0 \rangle} \cong \frac{i}{k}, \tag{12}$$

the last equality following by applying the so-called Wald approximation. Thus, the final result is

$$\Pr\{r_N \geq k | r_0 = i\} \cong \begin{cases} 0, & i = 0, \\ \frac{i}{k}, & 0 < i < k \\ 1, & i \geq k. \end{cases}, \tag{13}$$

Before proceeding, it is worth pointing out that (12) approximates the exact value with increasing precision as the expected value and the variance of the ray jumps x_n, $n \geq 1$, approaches zero and if x_n, $n \geq 1$, are identically distributed.

Finally, we substitute (10) and (13) into (6); after some manipulations, reported in the **Appendix B** of the companion paper [3], the ray-propagation through the lattice turns out to be fully described by means of the following closed-form relation:

$$\Pr\{r_N \geq k\} = p_1 \left[\sum_{i=1}^{k-1} \frac{i}{k} q_{e_i}^{+} \prod_{j=1}^{i-1} p_{e_j}^{+} + \prod_{j=1}^{k-1} p_{e_j}^{+} \right]. \tag{14}$$

As a check on the derived formula, note that it is independent of the status of the cells beyond row k, and that it reduces to the corresponding one obtained in [5] when $p_j = p$ for all j.

Equation (14) represents the natural way to extend the result in [5] to nonuniform density profiles. Nevertheless, at this point it makes sense to consider a slight modification of such a formula. Let us make reference to Figure 2 and let us focus on the evaluation of $\Pr\{r_N \geq k \,|r_0 = i\}$ when $0 < r_0 < k$. This corresponds to the problem of a one-dimensional discrete random walk with two absorbing barriers $r_{A1} = 0$ and $r_{A2} = k$, and we look for the probability that a walker, starting from level $r_0 = i$, is absorbed by the barrier $r_{A2} = k$ [Fig. $2(a)$] rather than $r_{A1} = 0$ [Fig. $2(b)$]. We explicitly note that these events are mutually exclusive, being $\Pr\{N = \infty\} = 0$. It is now evident that (12) estimates $\Pr\{r_N \geq k \,|r_0 = i\}$ on the basis of a distance criterion,

$$\Pr\{r_N \geq k \,|r_0 = i\} \cong \frac{\triangle_{A1}}{\triangle_{A1} + \triangle_{A2}} = \frac{i}{k}, \tag{15}$$

$\triangle_{A1}$ and $\triangle_{A2}$ being the distances between the starting level r_0 and the absorbing levels r_{A_1} and r_{A_2}, respectively. A little thought shows that such approximation does not take into account the fact that a ray traveling with negative direction inside the first level surely escapes from the grid, since there are not any occupied horizontal faces between level 1 and level 0 that can reflect the ray back into the grid. Accordingly, provided that $r_0 \geq 2$, the first absorbing barrier r_{A1} is not 0 but 1 and we define N as the number of reflections such that the ray either reaches (and eventually goes beyond) level k, $r_N \geq k$

[Fig. $2(c)$], or it is reflected back in the above empty half-plane crossing level 1, $r_N \leq 1$ [Fig. $2(d)$]. Applying the distance criterion, we obtain

$$\Pr\{r_N \geq k \,|r_0 = i\} \cong \frac{\triangle_{A1}}{\triangle_{A1} + \triangle_{A2}} = \frac{i-1}{k-1}. \tag{16}$$

Taking into account above considerations, we express $\Pr\{0 \longmapsto k\}$ as follows

$$\Pr\{0 \longmapsto k\} = \Pr\{0 \longmapsto 1 \prec 0\} \Pr\{1 \longmapsto k \prec 1\}, \tag{17}$$

where $\Pr\{0 \longmapsto 1 \prec 0\}$ is the probability that the ray reaches level 1 before being reflected back into level 0, i.e., the probability to enter the lattice, and $\Pr\{1 \longmapsto k \prec 1\}$ is the probability that the ray, starting from level 1, reaches level k, before being reflected back into level 1 and thus, escaping from the grid. The probability $\Pr\{0 \longmapsto 1 \prec 0\}$ is trivially equal to p_1, while $\Pr\{1 \longmapsto k \prec 1\}$ can be evaluated by following the same lines as in deriving (14) but taking into account a one-dimensional stochastic process defined starting from level 1 instead of level 0 [Fig. $1(b)$] and (16) instead of (15). This modification leads to the following result

$$\Pr\{0 \longmapsto k \prec 0\} = \begin{cases} p_1, & k = 1 \\ p_1 p_2 \left[\sum_{i=2}^{k-1} \frac{i-1}{k-1} q_{e_i}^{+} \prod_{j=2}^{i-1} p_{e_j}^{+} + \prod_{j=2}^{k-1} p_{e_j}^{+} \right], & k > 1 \end{cases} \tag{18}$$

that reduces to

$$\Pr\{0 \longmapsto k \prec 0\} = \begin{cases} p, & k = 1 \\ \frac{p^2 \left[1 - p_e^{(k-1)}\right]}{q_e (k-1)}, & k > 1 \end{cases} \tag{19}$$

when the uniform case is considered.

A key-issue should be pointed out. Equation (18) (as well as (14) and the analytical results obtained in [5]) holds true for a range of parameters to be accurately determined. This requires a mathematical analysis, carried out in the following section and assessed

by a numerical validation presented in Section 4.

3 On the Range of Applicability of the Martingale Approach

The final result (18), as well as (14), has been derived by assuming that the ray's jumps, successive to the first one, are independent and with zero-mean value (under such a condition the stochastic process $\{r'_n,\ n \geq 1\}$ can be considered a martingale with respect to $\{x_n,\ n \geq 1\}$). Moreover, accuracy of the Wald approximation increases if the mean and the standard deviation of the ray's jump x_n tend to zero and if the ray's jumps are identically distributed. Accordingly, we expect that (18) holds true when such properties are verified with reasonable accuracy. Hence, to evaluate the range of applicability of the proposed solution, we make some considerations on the distribution of x_n.

Before providing the mathematical formulation, we remind that the jump x_n starts at level r_{n-1}, where the n-th reflection takes place, and ends at level r_n, where the $(n+1)$-th reflection occurs. Since each jump can be either (a) in positive or (b) in negative direction, with probability $\Pr\{x_n = x_n^+\}$ and $\Pr\{x_n = x_n^-\}$ respectively, it follows that

$$\Pr\{x_n = i\} = \begin{cases} \Pr\{x_n = 0\,|x_n = x_n^+\}\Pr\{x_n = x_n^+\} & \\ \quad + \Pr\{x_n = 0\,|x_n = x_n^-\}\Pr\{x_n = x_n^-\} & , \quad i = 0, \\ \Pr\{x_n = i\,|x_n = x_n^+\}\Pr\{x_n = x_n^+\}, & i > 0, \\ \Pr\{x_n = i\,|x_n = x_n^-\}\Pr\{x_n = x_n^-\}, & i < 0. \end{cases} \tag{20}$$

Concerning the case $x_n = 0$, the ray hits a cell within the same level where the previous reflection has taken place. By means of the same arguments leading to (9), it turns out that

$$\Pr\left\{x_n = 0\,\middle|x_n = x_n^+\right\} = q^+_{e_{r_{(n-1)}}}. \tag{21}$$

The probability $\Pr\{x_n = 0\,|x_n = x_n^-\}$ can be easily obtained in the same way by taking

into account that the horizontal face encountered by the ray, which proceeds towards level $r_{(n-1)}$ with negative direction, is occupied with probability $q_{r_{(n-1)}-1}$. Accordingly,

$$\begin{aligned}\Pr\left\{x_n = 0 \,|x_n = x_n^-\right\} &= q_{r_{(n-1)}} \sum_{s=0}^{tan\theta-1} p_{r_{(n-1)}}^s + p_{r_{(n-1)}}^{tan\theta} q_{r_{(n-1)}-1} = \\ &= 1 - p_{r_{(n-1)}}^{tan\theta} p_{r_{(n-1)}-1} = 1 - p_{e_{r_{(n-1)}}}^- = q_{e_{r_{(n-1)}}}^-,\end{aligned} \tag{22}$$

where $p_{e_{r_{(n-1)}}}^-$ is the effective probability of the level $r_{(n-1)}$ to be freely crossed, given that the ray travels in the negative direction.

As far as remaining cases ($x_n \neq 0$) are concerned, we note that the ray crosses the generic level s either with probability $p_{e_s}^+$, if it is moving in positive direction, or with probability $p_{e_s}^-$, if it is proceeding in negative direction. Thus, with similar mathematics as for (10) we obtain

$$\Pr\left\{x_n = i,\ i > 0 \,\middle|\, x_n = x_n^+\right\} = q_{e_{r_{(n-1)}+i}}^+ \prod_{s=r_{(n-1)}}^{r_{(n-1)}+i-1} p_{e_s}^+ \tag{23}$$

and

$$\Pr\left\{x_n = i,\ i < 0 \,\middle|\, x_n = x_n^-\right\} = q_{e_{r_{(n-1)}+i}}^- \prod_{s=r_{(n-1)}+i+1}^{r_{(n-1)}} p_{e_s}^-, \tag{24}$$

respectively.

The evaluation of $\Pr\{x_n = x_n^+\}$ is now in order. Since the ray changes its direction of propagation only if it hits an horizontal face (Fig. 1), the ray travels with positive direction if an even number of the n total reflections occurs on horizontal faces of the lattice. Accordingly, we obtain

$$\Pr\left\{x_n = x_n^+\right\} = \sum_{i=0,even}^{n} \sum_{a_1=1}^{n-i+1} \sum_{a_2=a_1+1}^{n-i+2} \cdots \sum_{a_i=a_{i-1}+1}^{n} \sum_{c_n} \Pr\{c_n\} \prod_{s=1}^{i} \xi_h\left[a_s, r_{(a_s-1)}\right] \prod_{b=1, b\neq a_1,..,a_i}^{n} \xi_v\left[b, r_{(b-1)}\right]. \tag{25}$$

In (25) the indices a_s ($s = 1, ..., i$) and b can have any value between 1 and n and indicate the reflection number. The index $c_n = \left\{r_0,\ r_1,\ ...,\ r_{(n-1)}\right\}$ represents the sequence of levels where the n reflections take place. In (25) $\xi_h\left[a_s, r_{(a_s-1)}\right]$ is the probability of hitting an horizontal face at reflection a_s and at the corresponding level $r_{(a_s-1)}$, while $\xi_v\left[b, r_{(b-1)}\right]$

is the probability of hitting a vertical face at reflection b and at the corresponding level $r_{(b-1)}$. Both levels $r_{(a_s-1)}$ and $r_{(b-1)}$ are specified by the combination c_n.

Let us consider $\xi_h\left[j, r_{(j-1)}\right]$ and $\xi_v\left[j, r_{(j-1)}\right]$, i.e., the probabilities that the j-th reflection takes place on a horizontal and vertical face, respectively. Since at level $r_{(j-1)}$ the ray can hit at most one horizontal face (with occupancy probability either $q_{r_{(j-1)}+1}$ or $q_{r_{(j-1)}-1}$, depending on the direction) and $\tan\theta$ vertical faces (with occupancy probability $q_{r_{(j-1)}}$), we can assume that

$$\xi_h\left[j, r_{(j-1)}\right] = \begin{cases} \frac{q_{r_{(j-1)}+1}}{\tan\theta q_{r_{(j-1)}} + q_{r_{(j-1)}+1}}, & x_{(j-1)} = x^+_{(j-1)}, \\ \frac{q_{r_{(j-1)}-1}}{\tan\theta q_{r_{(j-1)}} + q_{r_{(j-1)}-1}}, & x_{(j-1)} = x^-_{(j-1)}. \end{cases} \tag{26}$$

In a similar way,

$$\xi_v\left[j, r_{(j-1)}\right] = \begin{cases} \frac{\tan\theta q_{r_{(j-1)}}}{\tan\theta q_{r_{(j-1)}} + q_{r_{(j-1)}+1}}, & x_{(j-1)} = x^+_{(j-1)}, \\ \frac{\tan\theta q_{r_{(j-1)}}}{\tan\theta q_{r_{(j-1)}} + q_{r_{(j-1)}-1}}, & x_{(j-1)} = x^-_{(j-1)}. \end{cases} \tag{27}$$

In (26) and (27) the direction that the ray is coming from depends on the previous jumps. Moreover, $\xi_h\left[j, r_{(j-1)}\right]$ and $\xi_v\left[j, r_{(j-1)}\right]$ depend on the occupancy probability at levels $r_{(j-1)}$, $r_{(j-1)}+1$ and $r_{(j-1)}-1$. Accordingly, we can not conclude that in general x_n's are independent of each other.

However, let us consider the situation where the occupancy probability between adjacent levels varies without abrupt changes. Under such an assumption, the approximation $q_{r_{(j-1)}} \cong q_{r_{(j-1)}+1} \cong q_{r_{(j-1)}-1}$ holds true and (26) and (27) take the form:

$$\xi_h\left[j, r_{(j-1)}\right] \cong \frac{1}{\tan\theta + 1} = \xi_h, \tag{28}$$

$$\xi_v\left[j, r_{(j-1)}\right] \cong \frac{\tan\theta}{\tan\theta + 1} = \xi_v. \tag{29}$$

It follows that the probability of hitting a horizontal or a vertical face is constant everywhere and everytime being independent from the level where the reflection takes place and

from the direction of propagation (and thus from the previous jumps). By substituting (28) and (29) into (25), we obtain

$$\Pr\left\{x_n = x_n^+\right\} \cong \sum_{i=0,even}^{n} \xi_h^i \xi_v^{n-i} \sum_{a_1=1}^{n-i+1} \sum_{a_2=a_1+1}^{n-i+2} \cdots \sum_{a_i=a_{i-1}+1}^{n} \sum_{c_n} \Pr\{c_n\}, \tag{30}$$

which reduces to

$$\Pr\left\{x_n = x_n^+\right\} \cong \sum_{i=0,even}^{n} \binom{n}{i} \xi_h^i \xi_v^{n-i} = \frac{1}{2}\left[1 + (\xi_v - \xi_h)^n\right] \hat{=} \alpha_n, \tag{31}$$

since $\sum_{c_n} \Pr\{c_n\} = 1$. Due to mutual exclusivity,

$$\Pr\left\{x_n = x_n^-\right\} \cong 1 - \alpha_n. \tag{32}$$

Accordingly, (20) can be written as

$$\Pr\{x_n = i\} \cong \begin{cases} \alpha_n q^+_{e_{r_{(n-1)}}} + (1-\alpha_n)\, q^-_{e_{r_{(n-1)}}}, & i = 0, \\ \alpha_n q^+_{e_{r_{(n-1)}+i}} \prod_{s=r_{(n-1)}}^{r_{(n-1)+i-1}} p^+_{e_s}, & i > 0, \\ (1-\alpha_n)\, q^-_{e_{r_{(n-1)}+i}} \prod_{s=r_{(n-1)}+i+1}^{r_{(n-1)}} p^-_{e_s}, & i < 0. \end{cases} \tag{33}$$

Thereafter, the x_n's distribution depends on n and θ, through α_n, and on the level $r_{(n-1)}$ where the n-th reflection occurred, as well as on the i adjacent levels.

At this point, a little thought shows that when θ is near to 45^o or a large number of reflections n occurs, $\Pr\{x_n = x_n^+\} \cong \Pr\{x_n = x_n^-\} \cong 1/2$. Thus, if the additional condition $q^+_{e_i} \cong q^-_{e_j}$, $i, j \geq 1$, holds true, it is easy to verify that in first approximation the hypothesis of independent, identically distributed and zero-mean jumps is satisfied. Moreover, as far as the condition on the standard deviation is concerned, it is easy to observe that, given an incidence condition, the standard deviation decreases as the occupancy probability q_j

for all j increases.

According to above mathematical considerations, we conclude that (18) faithfully describes the propagation process when ***(1)*** the incidence angle is not to far from the optimal value (i.e., $\theta \cong \theta_{opt} = 45^o$) or a large number of reflections takes place (i.e., $n \to \infty$), ***(2)*** the grid is dense, ***(3)*** the density profile does not present discontinuities and a significant variation in the levels of the lattice.

4 Numerical Validation

In order to assess the validity of the proposed solution and its range of applicability, as well as to provide a comparison with the Markov approach detailed in [3], an exhaustive set of numerical tests has been carried out. As a reference, results obtained by computer-based ray launching experiments, as described in [5], are reported.

In order to quantify the prediction accuracy of the proposed models with respect to the simulation, the values of the prediction error δ_k, the mean error $\langle\delta\rangle$, and the maximum error δ_{max} [3] are computed and compared. Moreover, in order to analyze the mean behavior when different density profiles are considered, the following figures are introduced as well:

$$\langle\delta_k\rangle \triangleq \frac{1}{I}\sum_{i=1}^{I}(\delta_k)_i\,, \quad (Global\ Prediction\ Error) \tag{34}$$

$$\langle\langle\delta\rangle\rangle \triangleq \frac{1}{K_{max}}\sum_{k=1}^{K_{max}}\langle\delta_k\rangle\,, \quad (Global\ Mean\ Error) \tag{35}$$

where $(\delta_k)_i$ are the values of the prediction error of the i-th profile and I is the total number of considered cases. Finally, to quantify the amount of variation of the density profile, let us introduce the *slope factor,* defined as:

$$S = \frac{|q_{MAX} - q_{MIN}|}{\triangle j}, \tag{36}$$

where q_{MAX} and q_{MIN} are the maximum and the minimum value of the occupancy prob-

ability, respectively, and $\triangle j$ is the number of levels over which such a variation occurs.

4.1 On the Role of the Obstacles Density

In this section, we analyze the effect of the obstacles density in the performance of the model [see condition **(2)** - Section 3]. The incidence angle is fixed, $\theta = \theta_{opt} = 45^o$, and uniform density profiles, having $q_j = q$ for all j, are considered.

With reference to Figure 3, it is clear that, as expected, accuracy of the MTG approach increases when dense random lattices are taken into account. As a matter of fact, the mean error ranges from 0.59%, when $q = 0.35$, up to 4.65%, when $q = 0.1$. It is worth noting that $\langle\delta\rangle_{q=0.4} > \langle\delta\rangle_{q=0.35}$. This can be easily explained by taking into account that, when $q = 1 - p = 0.4$, the probability that a site is free is approaching the percolating threshold $p_c \cong 0.59275$ [1]. It is well known that at this value the lattice suddenly changes its properties and for $q > q_c = 1 - p_c$ propagation is inhibited.

As far as the MKV approach is concerned, it provides more reliable predictions when sparse grids are considered. This allows to conclude that the two approaches are complementary. As a matter of fact, when $q \to 0$ the MTG approach evidently outperforms the MKV approach (as an example, $\left[\frac{\langle\delta\rangle_{MTG}}{\langle\delta\rangle_{MKV}}\right]_{q=0.1} \cong 9$), while when $q \geq 0.3$ the MTG approach allows a more faithful prediction (for instance, $\left[\frac{\langle\delta\rangle_{MKV}}{\langle\delta\rangle_{MTG}}\right]_{q=0.35} \cong 4$).

4.2 On the Role of the Variation Size in the Density Profile

This section gives a quantitative meaning to the condition **(3)** in Section 3, according to which lower variation in the density profile leads to more accurate results. We fix the incidence angle $\theta = \theta_{opt} = 45^o$ and we take into account several decreasing linear density profiles,

$$q_j = q - \alpha(j - 1), \tag{37}$$

q being equal to 0.35. The values of the parameter α, that in this case corresponds to the slope factor S, are reported in Table I.

With reference to Table I and to Figure 4, it can be noticed that, as expected, the prediction accuracy of the MTG approach decreases as S grows. In particular, $\langle\delta\rangle$ ranges from 0.35%, when $S = 1.61 \times 10^{-3}$, up to 2.88% when $S = 9.68 \times 10^{-3}$. Such a behavior points out the sensitivity of the MTG approach with respect to the slope factor S ($\frac{\max\langle\delta\rangle}{\min\langle\delta\rangle} \cong 8$). On the other hand, it is evident that the performance of the MKV approach is not affected by the slope factor ($\frac{\max\langle\delta\rangle}{\min\langle\delta\rangle} \cong 1$), as pointed out in [3]. Thus, while the MTG approach outperforms the MKV approach in describing propagation in the dense slowly variable profiles (i.e., L1, L2, L3 and L4), the MKV approach gives better predictions for high S values.

4.3 On the Role of the Density Profile Type

In this section, we analyze the dependence of the prediction accuracy on the type of the density profile. According to the considerations drawn at the end of Section 3 and the results obtained in the previous test case, we expect that the MTG approach satisfactorily performs for all density profiles characterized by a low S value and with high occupancy probability throughout the whole lattice. The incidence angle is fixed, $\theta = \theta_{opt} = 45^o$, and two slowly variable dense profiles, having $0.3 \leq q_j \leq 0.4$ for all j, and $S = 6.25 \times 10^{-3}$, are considered, namely a double-exponential density profile (DE),

$$q_j = \begin{cases} \alpha \exp\left[(j-L)\tau\right] & j \leq L \\ \alpha \exp\left[(L-j)\tau\right] & j > L \end{cases}, \tag{38}$$

having $\alpha = 0.4$, $L = K_{max}/2 = 16$ and $\tau = 17.98 \times 10^{-3}$, and a pseudo-gaussian density profile (PG),

$$q_j = \alpha \exp\left\{-\frac{(j-L)^2}{\sigma^2}\right\}, \tag{39}$$

having $\alpha = 0.4$, $L = K_{max}/2 = 16$ and $\sigma = 29.83$.

Mean error $\langle\delta\rangle$ and maximum error δ_{max} values obtained by applying the MTG approach and the MKV approach are reported in Table II. As expected, the MTG approach allows

reliable predictions and outperforms the MKV approach ($\langle\delta\rangle_{MKV} \cong [\delta_{max}]_{MTG}$). Moreover, as far as the MTG approach is concerned, it is interesting to observe that $\langle\delta\rangle$ values are comparable with respect to each other and with respect to the $\langle\delta\rangle$ value obtained for the decreasing linear profile L4, see Table I, that is characterized by a slope factor of the same magnitude ($S_{L4} = 6.45 \times 10^{-3}$). This further confirms that the MTG performances are affected by the variation in the density profile, pointing out as well their independence on the complexity of the obstacles density profile in hand.

4.4 On the Role of the Incidence Angle

Finally, an analysis of the dependence of the prediction effectiveness on the incidence angle θ has been carried out [condition ***(1)*** - Section 3]. We consider dense profiles without abrupt discontinuities and without high variation along the lattice depth (i.e., obstacles density profiles satisfying conditions ***(2)*** and ***(3)*** [Section 3]).

With reference to Figure 5, that plots the global mean error $\langle\langle\delta\rangle\rangle$ versus θ for uniform profiles having q equal to 0.3, 0.35 and 0.4, several observations can be drawn. First of all, it is evident that while for $\theta = 75^o$ the performances of the two approaches are comparable, for the other θ values the MTG approach evidently outperforms the MKV approach. Moreover, as expected, both approaches lose accuracy when θ deviates from the optimal value $\theta_{opt} = 45^o$. However, it is interesting to observe that while the MKV performances evidently depend only on the distance $|\theta - \theta_{opt}|$, the MTG approach is affected by the current θ value. In particular, for a fixed distance value, we observe that the mean error returned by the MTG approach is lower in correspondence with the higher θ value (for instance, when $|\theta - \theta_{opt}| = 30^o$, $\langle\langle\delta\rangle\rangle = 4.49\%$ when $\theta = 15^o$ and $\langle\langle\delta\rangle\rangle = 1.68\%$ when $\theta = 75^o$). This can be easily explained by taking into account that, in order ensure reliable predictions, the MTG approach requires either the incidence angle to be near the optimal value $\theta_{opt} = 45^o$ or a large number of reflections to take place [condition ***(1)*** - Section 3]. Now, for fixed k and q values, when $\theta \to 90^o$ the average number of reflections n is expected to be larger and condition ***(1)*** tends to be satisfied even if $|\theta - \theta_{opt}|$ is far

from zero. This is further confirmed by Figure 6, where plots of the global prediction error $\langle \delta_k \rangle$ are shown. Let us focus on the MTG approach and the case $|\theta - \theta_{opt}| = 30^o$. While in the first levels the values $\langle \delta_k \rangle_{\theta=75^o}$ and $\langle \delta_k \rangle_{\theta=15^o}$, when $\theta = 75^o$ and $\theta = 15^o$, are comparable, by increasing k, $\langle \delta_k \rangle_{\theta=75^o}$ reduces with respect to $\langle \delta_k \rangle_{\theta=15^o}$ and it turns out to be comparable with $\langle \delta_k \rangle_{\theta=45^o}$.

The same considerations outlined by taken into account uniform density profiles hold true when dense nonuniform profiles are considered, as confirmed by the global mean error $\langle \langle \delta \rangle \rangle$ values obtained for profiles L1, DE and PG (see Tab. III).

5 Conclusions

The problem of ray propagation in a nonuniform random lattice has been addressed. The present contribution builds upon the companion paper [3], where an approach based on the theory of the Markov chains has been presented and compared with the result in [5] and to its extension to the nonuniform case, referred to as Martingale approach. Here, the whole theory concerning the Martingale approach, including a deep analysis on its range of validity, has been presented and an innovative modification, leading to improved results, has been introduced. Numerical experiments have confirmed the feasibility of the proposed approach in dealing with ray propagation in nonuniform random lattices, as well as revealing its limitations and allowing a comparison with the Markov approach.

With reference to the results presented in both the present contribution and in the companion paper, we conclude that the Markov and the Martingale approaches are complementary when dealing with ray propagation in random lattices. In particular, the Martingale approach is to be preferred when dense, slowly variable density profile are taken into account, while the Markov approach returns better predictions when sparse or highly variable profiles are at hand. As far as the incidence angle θ is concerned, both approaches lose accuracy when the incidence angle deviates from 45^o, although the MTG approach returns reliable predictions also for high θ values, provided that k and

the obstacles density are high enough.

Appendix A

This section is devoted at proving that, under the assumption of independent and zero-mean jumps, the process$\{r'_n,\ n \geq 1\}$ is a martingale with respect to $\{x_n,\ n \geq 1\}$.
According to the definition provided in [6], in order to be considered as a martingale random process, $\{r'_n,\ n \geq 1\}$ must satisfy the following conditions:

$$\begin{cases} \langle |r'_n| \rangle < \infty, & (i) \\ \left\langle r'_{n+1} | x_n, x_{n-1}, ..., x_1 \right\rangle = r'_n. & (ii) \end{cases}$$

As far as the condition (i) is concerned, we observe that

$$\langle |r'_n| \rangle \leq \sum_{i=1}^{n} \langle |x_i| \rangle$$

and

$$\langle |x_i| \rangle \leq \left\langle |x_i^{MAX}| \right\rangle,$$

where $|x_i^{MAX}|$ is a geometric random variable of parameter q_e^{MAX}, with $q_e^{MAX} = 1 - p_e^{MAX}$, $p_e^{MAX} = \max_j \left\{ p_{e_j}^+, p_{e_j}^- \right\}$. Therefore, it turns out that

$$\left\langle |x_i^{MAX}| \right\rangle = \frac{p_e^{MAX}}{q_e^{MAX}}.$$

If $p_e^{MAX} < 1$ then

$$\langle |r'_n| \rangle \leq \sum_{i=1}^{n} \langle |x_i| \rangle \leq \sum_{i=1}^{n} \left\langle |x_i^{MAX}| \right\rangle = n \frac{p_e^{MAX}}{q_e^{MAX}} < \infty.$$

Otherwise, if $p_e^{MAX} = 1$ to avoid trivialities (i.e., $q_j = 0$, $\forall j$), it is needed that

$$\sum_{i=1}^{n} \langle |x_i| \rangle < \sum_{i=1}^{n} \left\langle |x_i^{MAX}| \right\rangle$$

and consequently

$$\langle |r'_n| \rangle < \infty.$$

Concerning the condition (ii), by considering the assumption of independent and zero-mean jumps, then

$$\begin{aligned} \left\langle r'_{n+1} | x_n, x_{n-1}, ..., x_1 \right\rangle &= \langle r'_n + x_{n+1} | x_n, x_{n-1}, ..., x_1 \rangle \\ &= \langle r'_n | x_n, x_{n-1}, ..., x_1 \rangle + \langle x_{n+1} | x_n, x_{n-1}, ..., x_1 \rangle \\ &= r'_n + \langle x_{n+1} \rangle = r'_n. \end{aligned}$$

Correction to the Companion Paper

In [3] there was a typographical error in Eq. (26). The correct equation should read:

$$\Pr\{r_0 = i\} = \begin{cases} q_1, & i = 0, \\ p_1 q_{e_i}^{+} \prod_{j=1}^{i-1} p_{e_j}^{+}, & i \geq 1. \end{cases}$$

Acknowledgments

This work has been supported in Italy by the "*Progettazione di un Livello Fisico 'Intelligente' per Reti Mobili ad Elevata Riconfigurabilità*," Progetto di Ricerca di Interesse Nazionale - Miur Project COFIN 2005099984, and in U.S. in part by the National Scienc Foundation CAREER award CNS-0546235.

Author Contact Information

Corresponding author Andrea Massa may be reached at the address on the title page, by phone at +39-0461-882057, fax at +39-0461-882093, or e-mail at andrea.massa@ing.unitn.it.

References

[1] G. Grimmett, *Percolation*. Springer-Verlag, New York, 1989.

[2] D. Stauffer, *Introduction to Percolation Theory*. Taylor and Francis, London, 1985.

[3] A. Martini, M. Franceschetti, and A. Massa, "Ray propagation in nonuniform random lattices," *J. Opt. Soc. Am. A*, **23**, 2251-2261, 2006.

[4] J. R. Norris, *Markov chains*. Cambridge U. Press, 1998.

[5] G. Franceschetti, S. Marano, and F. Palmieri, "Propagation without wave equation toward an urban area model," *IEEE Trans. Antennas Propag.*, **47**, 1393-1404, 1999.

[6] R. M. Ross, *Stochastic Processes*. J. Wiley, New York, 1983.

Tables

Table I. Linear density profiles. Parameter α and mean error $\langle\delta\rangle$ values when $\theta = 45^o$.

Profile	L1	L2	L3	L4	L5	L6
$\alpha\ [\times 10^{-3}]$	1.61	3.23	4.84	6.45	8.06	9.68
$\langle\delta\rangle_{MTGA}$	0.35	0.73	1.26	1.75	2.34	2.88
$\langle\delta\rangle_{MKVA}$	2.12	2.09	1.98	1.95	1.84	1.82

Table II. Double-exponential (DE) and pseudo-gaussian (PG) density profiles. Mean error $\langle\delta\rangle$ and maximum error δ_{max} values when $\theta = 45^o$.

	Profile DE		Profile PG	
	MTG	MKV	MTG	MKV
$\langle\delta\rangle$	1.35	2.42	1.31	2.16
δ_{max}	2.17	2.96	2.26	2.87

Table III. Nonuniform density profile L1, DE and PG. Global mean error $\langle\langle\delta\rangle\rangle$ values obtained for different incidence angles θ.

θ	15^o	30^o	45^o	60^o	75^o
$\langle\langle\delta\rangle\rangle_{MTGA}$	5.26	3.56	1.01	1.84	1.79
$\langle\langle\delta\rangle\rangle_{MKVA}$	4.62	4.06	2.23	4.12	4.10

Figure Captions

- **Figure 1.** Vectorial representation of the stochastic process modeling ray propagation inside nonuniform random lattices. The n-th element of the stochastic process r_n is the vertical component of the vector $\bar{r}_n$.

- **Figure 2.** The two mutually exclusive situations at reflection $n = N$, (a)-(b) N being $\min\{n :\ r_n \geq k \ or \ r_n \leq 0\}$ and (c)-(d) N being $\min\{n :\ r_n \geq k \ or \ r_n \leq 1\}$.

- **Figure 3.** Uniform random lattices - Mean error $\langle\delta\rangle$ for different q values when $\theta = 45^o$.

- **Figure 4.** Linear density profiles, $q_j = q - \alpha(j-1)$, $q = 0.35$, α values specified in Table I - Prediction error δ_k versus k when $\theta = 45^o$. Left-hand side, MTG approach; right-hand side, MKV approach.

- **Figure 5.** Uniform random lattices, $q = \{0.3, 0.35, 0.4\}$ - Global mean error $\langle\langle\delta\rangle\rangle$ for different incidence angles θ.

- **Figure 6.** Uniform random lattices, $q = \{0.3, 0.35, 0.4\}$ - Plots of the global prediction error $\langle\delta_k\rangle$ versus k for different incidence angles θ. Left-hand side, MTG approach; right-hand side, MKV approach.

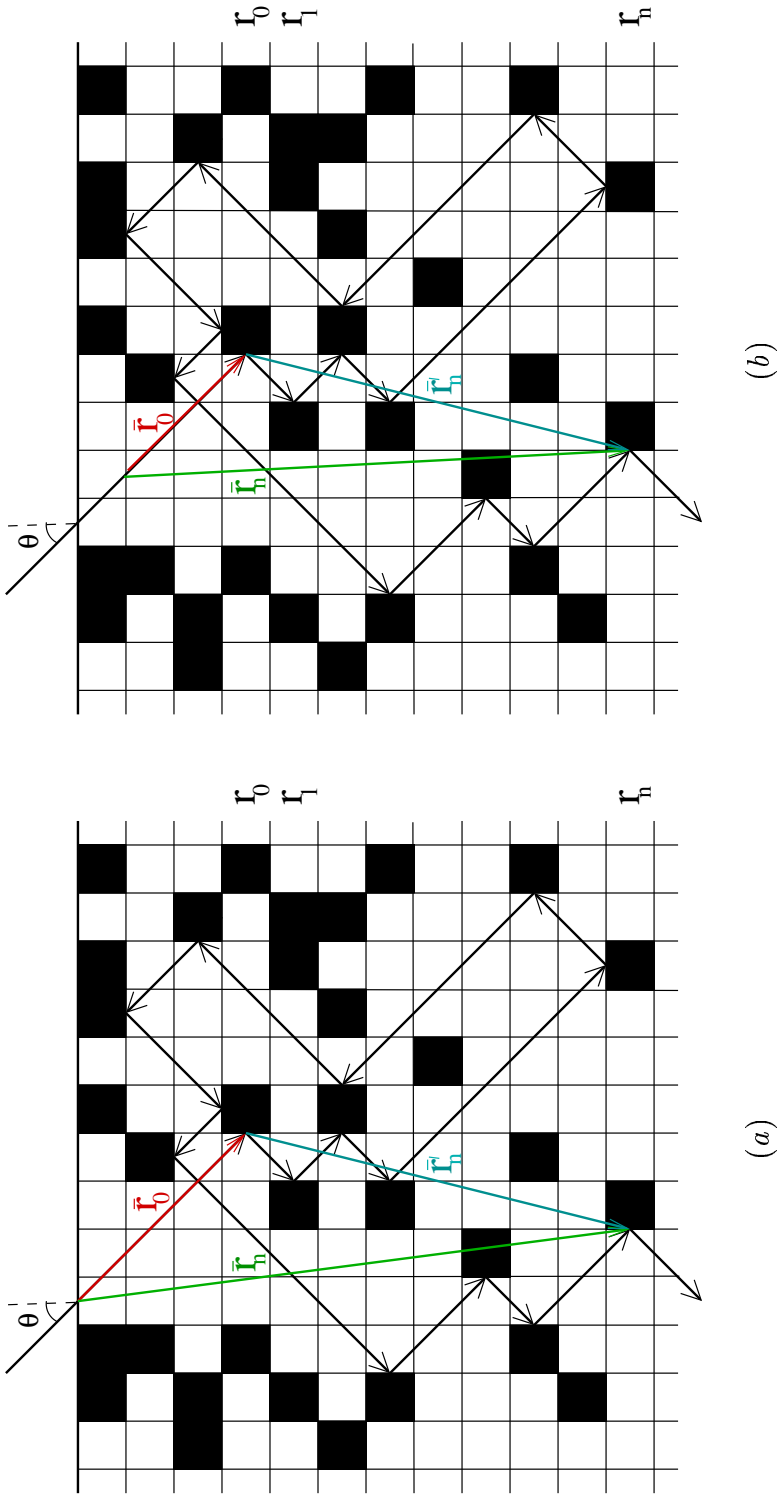

Fig. 1 - A. Martini *et al.*, "Ray propagation in nonuniform random lattices - Part II"

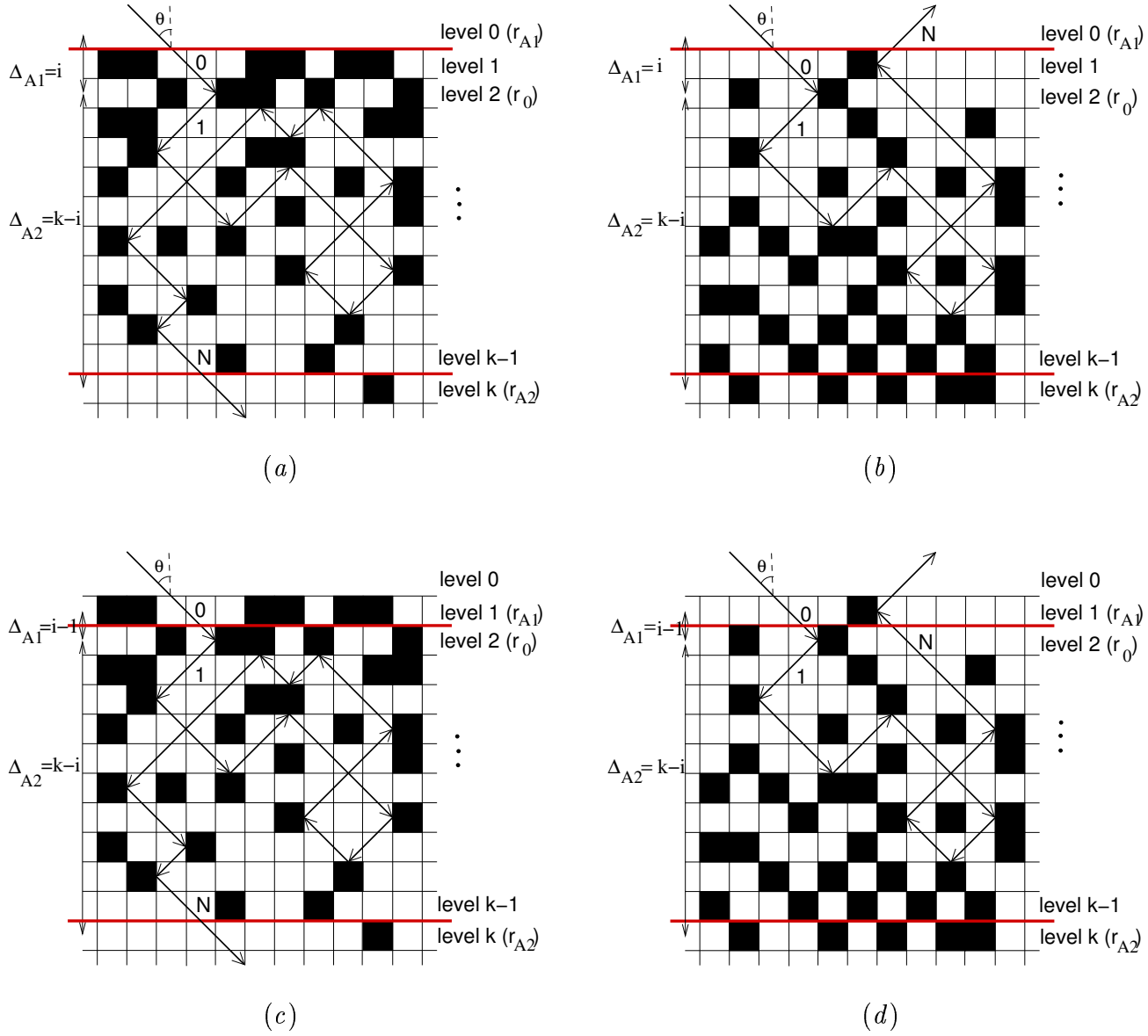

Fig. 2 - A. Martini *et al.*, "Ray propagation in nonuniform random lattices - Part II"

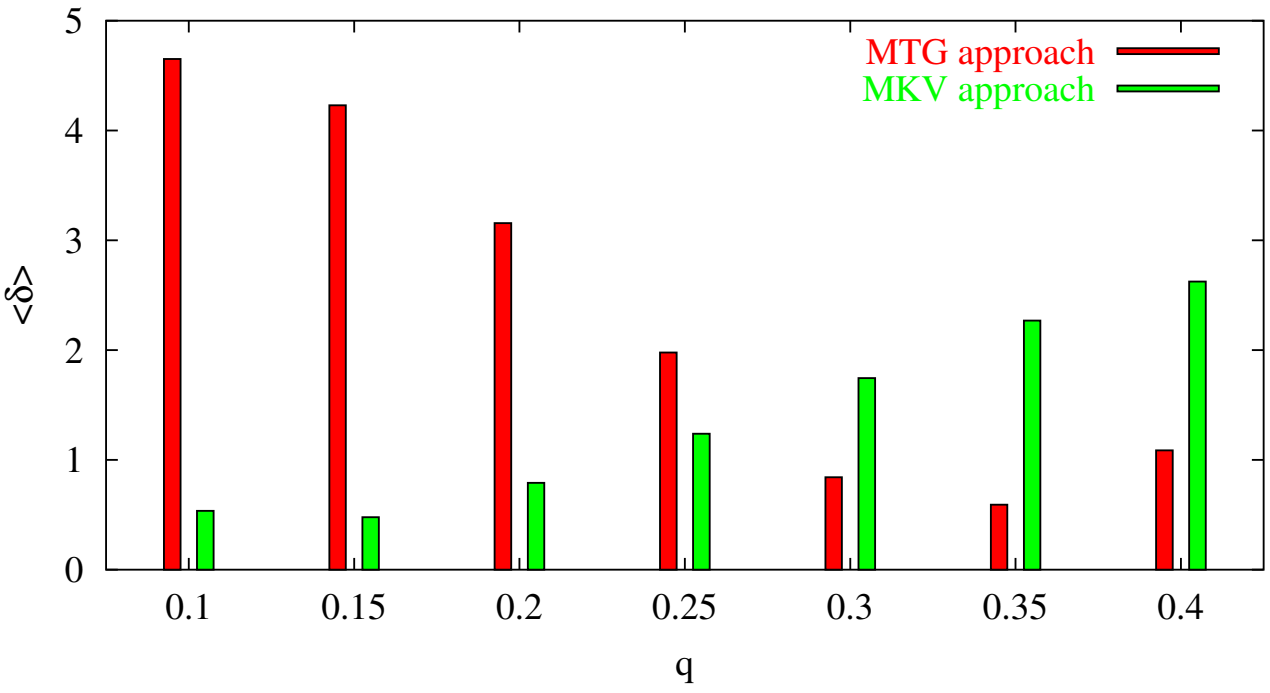

Fig. 3 - A. Martini *et al.*, "Ray propagation in nonuniform random lattices - Part II"

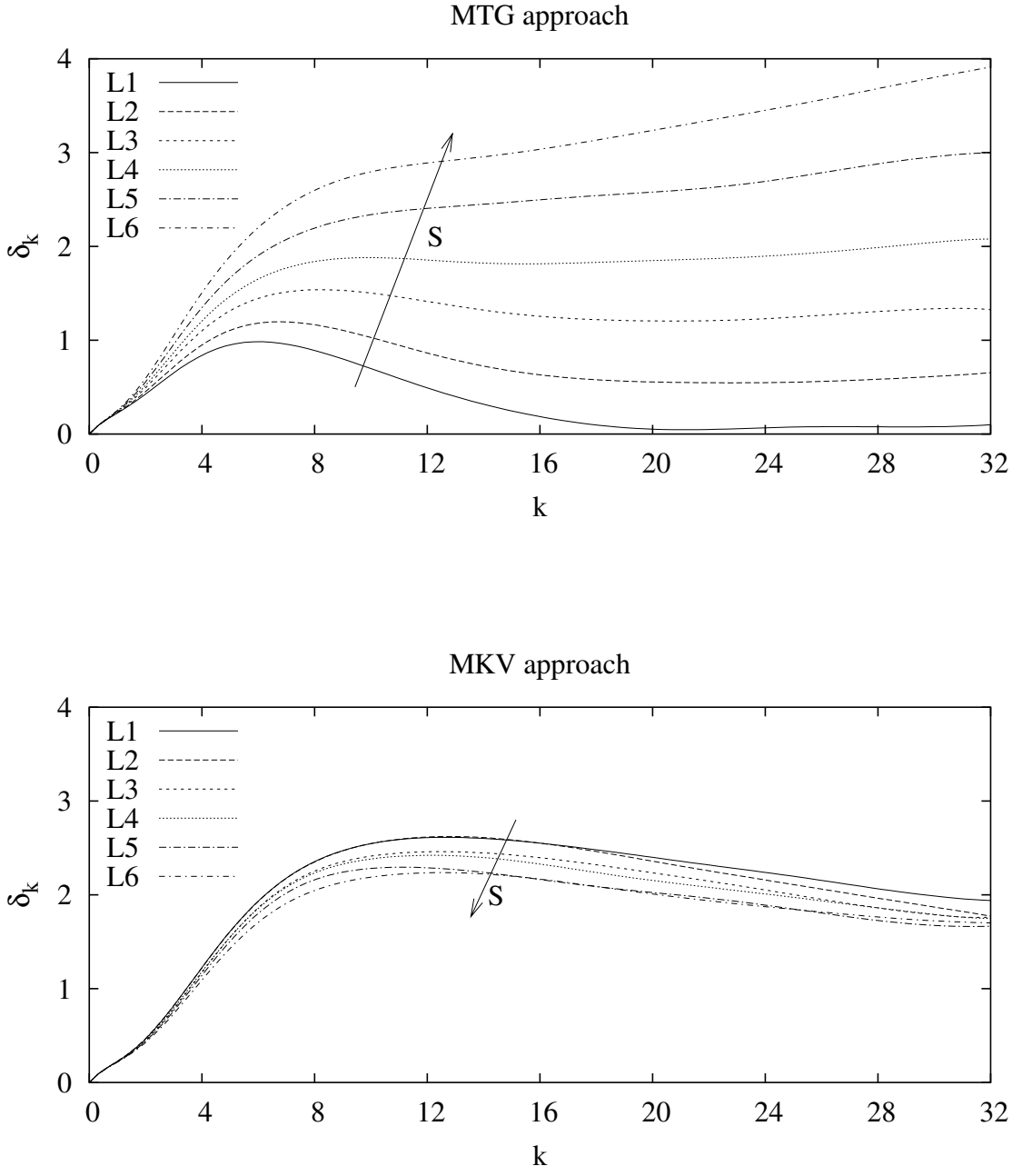

Fig. 4 - A. Martini *et al.*, "Ray propagation in nonuniform random lattices - Part II"

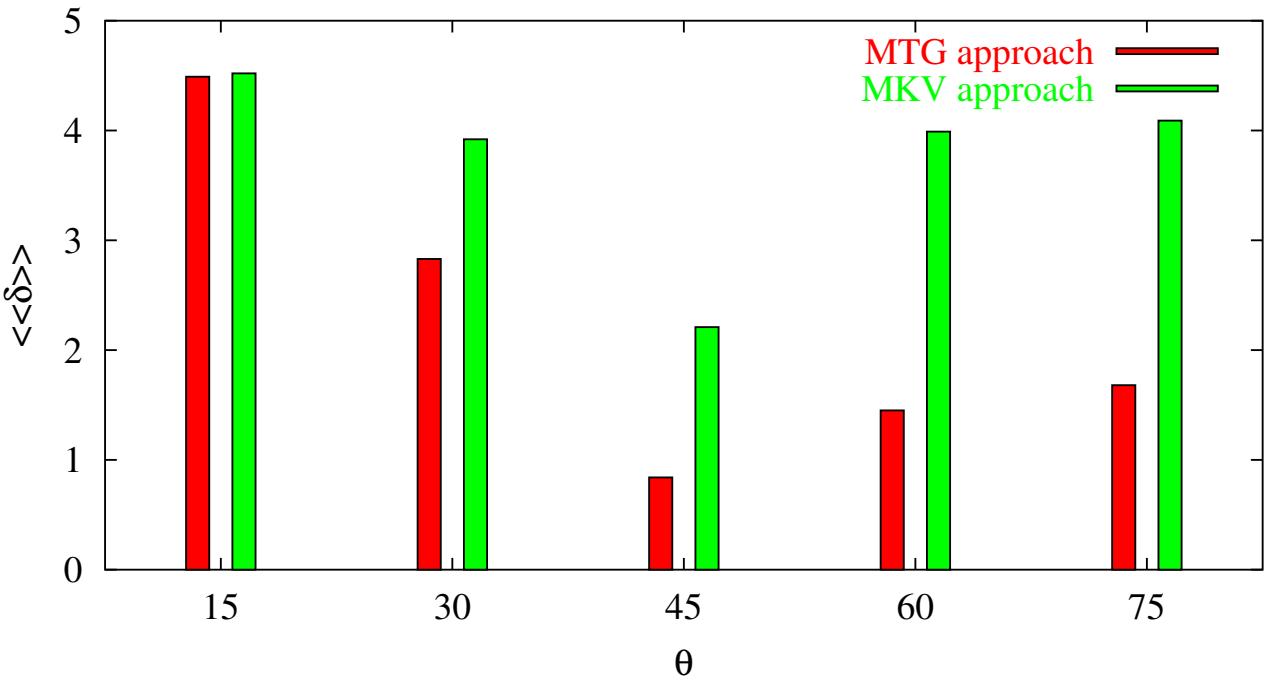

Fig. 5 - A. Martini *et al.*, "Ray propagation in nonuniform random lattices - Part II"

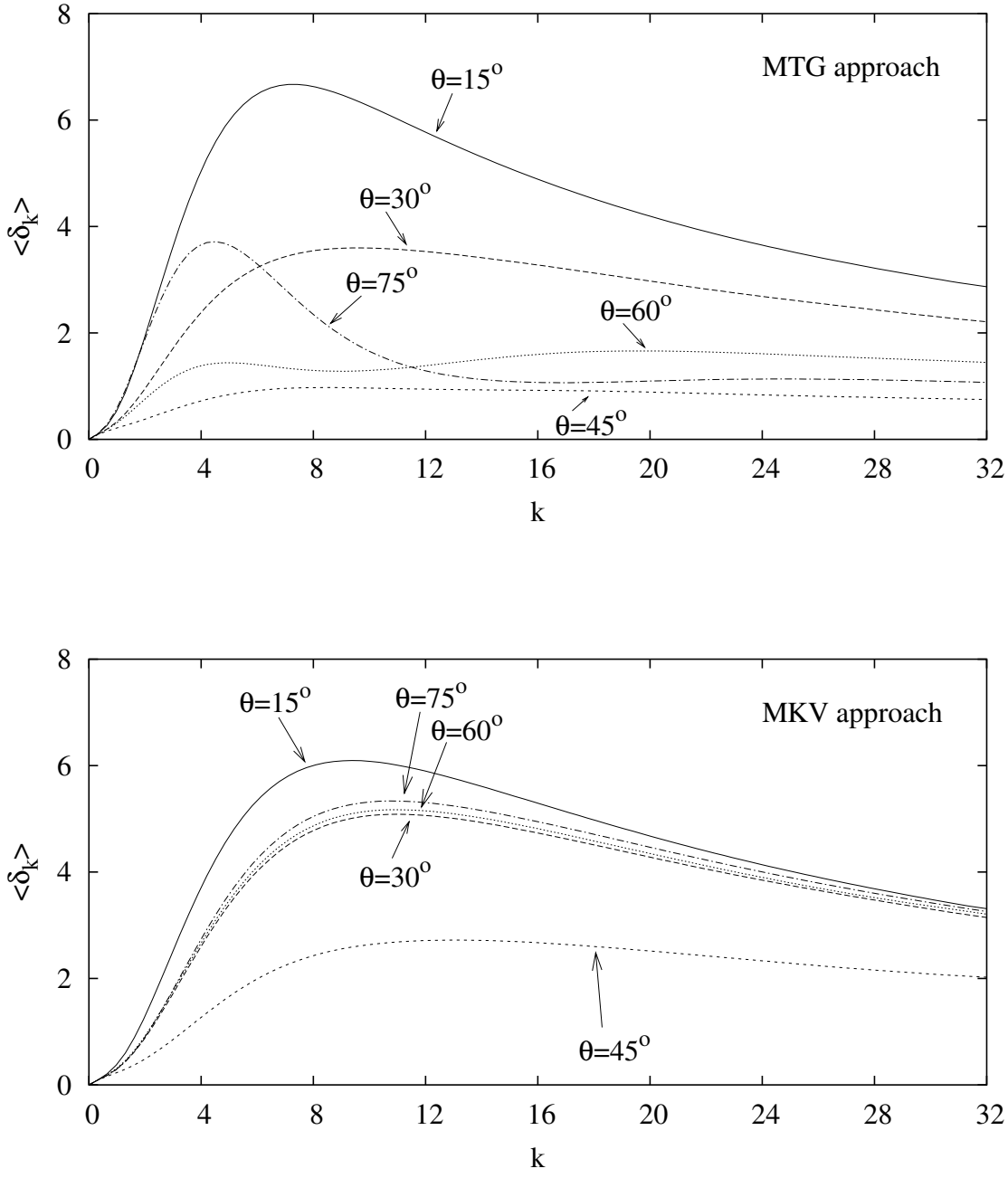

Fig. 6 - A. Martini *et al.*, "Ray propagation in nonuniform random lattices - Part II"